Numerical optimization of active heat sinks considering restrictions of selective laser melting

F. Lange[1], C. Hein[1], G. Li[1], C. Emmelmann[1,2]
1. Fraunhofer Research Institution for Additive Manufacturing Technologies IAPT, Hamburg, Germany
2. Institute of Laser and System Technologies, Hamburg University of Technology, Germany

Abstract

Parametric and topology optimization approaches are widely used techniques for performance improvement of components in terms of various objectives. Especially topology optimization often leads to complex geometries that are difficult or impossible to be produced by conventional manufacturing processes. Due to its great freedom in shape and structure design, additive manufacturing methods like selective laser melting are predestined for the production of such components. Nonetheless some restrictions need to be considered while designing parts for additive manufacturing to ensure for example the printability or the possibility to remove support structures. In this paper, an optimized design of an active heat sink is sought. The goal of the optimization is the maximization of the thermal conductivity, hence the minimization of the temperature of the heat dissipating component. Therefore, a parametric as well as a topology optimization is implemented in COMSOL Multiphysics® and compared to each other in terms of performance improvement and computational effort. The heat transfer in solids module in combination with the optimization module is used for the two-dimensional calculations. Manufacturing restrictions are included into the simulations to directly obtain printable components granting a reduction of post processing effort. Limitations of such restrictions are shown and approaches to handle these limitations are investigated. Experiments with 3D-printed prototypes are carried out in order to validate the numerical results. In comparison, a conventional heat sink is investigated to show lightweight potentials and possibilities of performance improvement.

Keywords

topology optimization, parametric optimization, heat sink, convective cooling, 3D printing, additive manufacturing

1. Introduction

Electronic devices like LEDs or computer chips dissipate heat because of thermal losses. In applications with high requirements regarding the weight and build space as the automotive or aerospace industry, small and light weight heat sinks are needed for cooling. Topology optimization methods are nowadays investigated for improved heat sinks designs with better thermal performances and lower pressure drops. [1–5] Compared to conventional design based on the engineer's skills and experience, topology optimization [6] is a systematic approach which can lead to unintuitive and innovative designs.

Additive manufacturing methods like the selective laser melting are used for the manufacturing of complex topology optimized structures because of the great design freedom provided by a tool-free, layer-wise production. [7] This design freedom also allows for compact designs of thermal components with good adaptation to geometrical boundary conditions. [8, 9]

Even though 3D printing grants great freedom in shape and structural design, the restrictions of additive manufacturing need to be considered during the design phase of components. [10, 11] These restrictions strongly differ from conventional processes, are highly material dependent and have to be adjusted for any change in printing material or even alloy. The minimum wall thickness for example is amongst others limited by the radius of the laser beam. [12]

Manufacturing restrictions can be directly integrated into topology optimization simulations, to only generate geometries fitting this constraints. Some of these restrictions have already been successfully implemented, like wall thickness restrictions [13], overhang constraints [14] as well as cavity problems [15]. In comparison, the benefit of a parametric optimization is the easy imple-

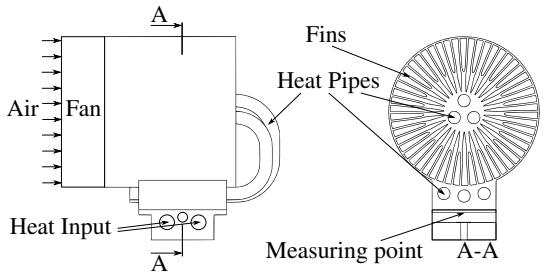

Figure 1. Definition of the problem.

mentation and exact limitation of the design variables. Thus, parameters like the wall thickness can be easily restricted to minimum values.

In this paper a parametric optimization and a topology optimization approach are compared for an active heat sink with three heat pipes (see Figure 1) regarding the thermal performance and the computational effort.

The results of the optimization are evaluated with an experimental setup where the optimized and additive manufactured heat sinks are tested along with a conventional heat sink. To ensure comparability between the investigated optimization results the same alloy AlSi10Mg was used to print all heat sink prototypes.

2. Governing Equations

The problem to be solved is a standard nonlinear optimization problem of the form

$$\begin{aligned} &\text{minimize } f_0(x) \\ &\text{subject to } f_i \leq 0 \qquad\qquad i = 1,\ldots,m, \\ &\qquad x_j^{\min} \leq x_j \leq x_j^{\max}, \quad j = 1,\ldots,n. \end{aligned} \tag{1}$$

where f_0 is the objective function, f_i are behavior constraints, m is the number of constraints, and x is a vector of n design variables, x_j. [16–18]

For the numerical analysis of the heat transfer, solutions are found for the governing conservation equation of energy. For steady state the heat transfer is given by Fourier's Law

$$-\nabla \cdot (k\nabla T) = Q, \tag{2}$$

where k is the thermal conductivity, T is the Temperature state variable and Q is the volumetric heat generation. Since the fluid flow is not considered, the general objective function, $f_{0,\,\mathrm{par}}$, in this optimization problem is equivalent to minimizing the total variation of the temperature in the design domain Ω during a constant heat generation, which is analogical to maximizing the thermal conductivity of the domain [1]:

$$f_{0,\,\mathrm{par}} = \int_\Omega k\,(\nabla T)^2\,\mathrm{d}\Omega. \tag{3}$$

2.1 Parametric Optimization

Additionally, a restriction of a limited area fraction of the form

$$\int_\Omega A_{\mathrm{fins}}\mathrm{d}\Omega < \gamma_0 A_\Omega \tag{4}$$

with the area of the fins A_{fins}, the area of the design domain A_Ω and the material fraction γ_0 is applied for the parametric optimization. The Bound Optimization BY Quadratic Approximation (BOBYQA) algorithm is used to solve this optimization problem. [18]

2.2 Topology Optimization

In order to find the optimal topology for given objective functions and constraints, the material distribution method is used. For this purpose a design variable (design density ρ_{des}) is defined which takes values between 0 (no material or fluid) and 1 (solid material) for each finite element. A so called 'penalization' scheme is used to influence the material distribution such that intermediate design values are repressed and a well defined material distribution is achieved, see [19]. The objective function is defined analogous to the parametric optimization

$$f_{0,1} = \int_\Omega k_{\mathrm{SIMP}}\,(\nabla T)^2\,\mathrm{d}\Omega. \tag{5}$$

where k_{SIMP} is the thermal conductivity as a function of ρ_{des} by applying the solid isotropic material with penalization (SIMP) rule [4, 6]:

$$k_{\mathrm{SIMP}}(\rho_{\mathrm{des}}) = (k_{\mathrm{s}} - k_{\min}) \cdot \rho_{\mathrm{des}}^n + k_{\min} \tag{6}$$

with the thermal conductivity of the solid material k_{s} and the minimal value of thermal conductivity $k_{\min}$ which is chosen to be much smaller than k_{s} and n is the penalization factor. Since an active

cooling with air is intended, a limit on the solid fraction γ of the domain area A is introduced by

$$0 \leq \int_{\Omega} \rho_{\mathrm{des}}(x)\,\mathrm{d}\Omega \leq \gamma A, \tag{7}$$

to allow the fluid to pass by. The total variation of the design variable is used to define a problem- and mesh-independent dimensionless penalty term for intermediate densities of the form [13]

$$f_{0,2} = \frac{h_0 h_{\max}}{A} \int_{\Omega} |\nabla \rho_{des}(x)|^2 \mathrm{d}\Omega \tag{8}$$

where h_0 is the parameter governing the size of details in the solution and $h_{\max}$ is the actual mesh size. The parameter h_0 can be used to adjust Equation 8 such that it fits the manufacturing restrictions for minimum wall size.

The final objective function is received by balancing the objective and penalty term against each other. Therefore, a linear combination controlled by the parameter q of the form

$$\begin{aligned} f_0 = \quad & (1-q)\int_{\Omega} k_{\mathrm{SIMP}}(\nabla T)^2\,\mathrm{d}\Omega \\ & + q\tfrac{h_0 h_{\max}}{A}\int_{\Omega} |\nabla \rho_{des}(x)|^2 \mathrm{d}\Omega \end{aligned} \tag{9}$$

is chosen. q defines the weighting of the different objectives against each other. $f_{0,1}$ tempts to create long, narrow and pointed ramifications. This works against the restriction of a given minimum wall thickness $f_{0,2}$. Thus, the minimum wall thickness is respected in a global scope, while it is locally violated - especially at the end of narrow branches. This results in structures that are not printable, because the laser diameter is greater than the structure itself.

3. Computational Model

3.1 Parametric Model

The geometric composition for the parametric optimization is abstracted from topology optimization results known from the literature, [4, 5]. The boundary conditions, the mesh and the design variables for the parametric optimization are shown in Figure 2. In addition, the cross section area was limited to a value of 30% of the simulation domain, to keep the weight of the component as small as possible and to enable a free fluid flow between the fins. Furthermore the number of the fins is also a design variable for the optimization,

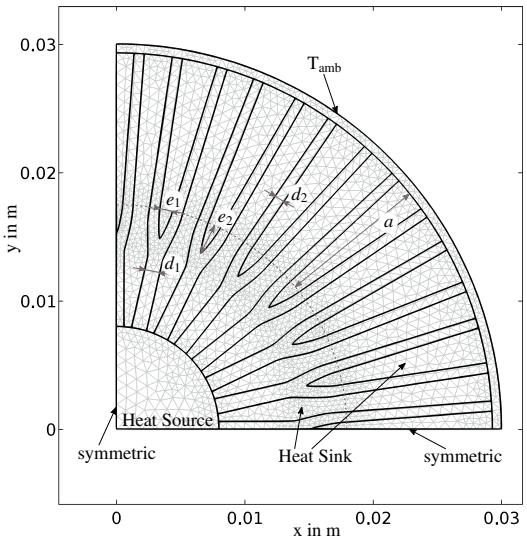

Figure 2. Used parameters, the mesh and boundary conditions for the two-dimensional parametric optimization. There are symmetric conditions at all boundaries at the left and bottom side. The outer boundary is assumed to be at ambient temperature ($T_{\mathrm{amb}} = 293.15\,\mathrm{K}$).

so that there are six variables to vary. Some constraints are applied to these variables, like d_1 and d_2 are restricted by the minimum wall thickness, compare to [10], and the other ones by geometric limitations.

A maximum element size of $1 \times 10^{-3}\,\mathrm{m}$ is chosen which results in 4330 to 6800 elements depending on the number of fins and the current parameter set. Due to the symmetry of the problem only a quarter of the component is simulated, this goes along with a simplification of the heat source, compare Figures 1 and 2 or 3, but ensures a comparability of the different approaches.

3.2 Topological Model

A two-dimensional, stationary simulation with respect to the material distribution method is performed. A mesh of tetrahedral elements is used for the discretization of the simulation domain. The maximum element size in the domain is varying between $1 \times 10^{-4}\,\mathrm{m}$ in the design space to $2 \times 10^{-4}\,\mathrm{m}$ in the solid areas at the borders of the design space.

The simulation domain with the design space for the topology optimization, as well as the boundary conditions and mesh are shown in Figure 3. The boundary conditions and the values of the

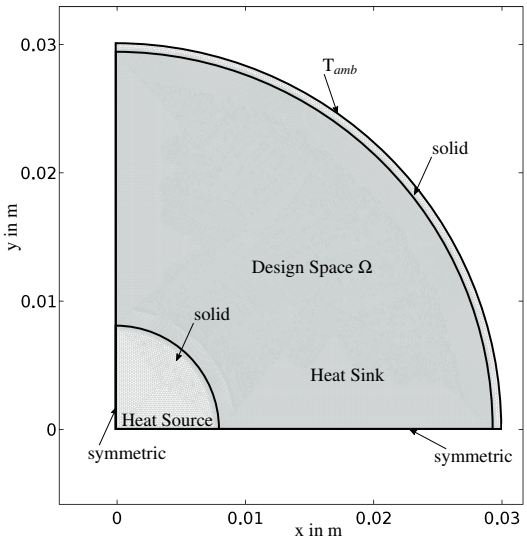

Figure 3. The boundary conditions of the two-dimensional simulation domain are shown. A heat source in the center of the simulation domain and the heat sink in the design space represent respectively the heat transferred by the heat pipes into the system and the heat carried away by the fluid.

heat source and heat sink are chosen analogous to the parametric model. In order to unfold the whole potential of additive manufacturing, the part should be in one piece, to avoid an assembling of the component. To ensure that, optimized structures have to be connected to the outer wall. Thus the value of the heat source is chosen to be greater than the value of the heat sink, so that excessive energy is forced to be dissipated over the solid casing.

4. Optimization Results

4.1 Parametric Model

The results of the parametric optimization are shown in Table 1. The solver attempts to use as many fins as possible, because of a homogenization of the temperature field, compare with Figure 4. However, due to the limitation of the solid area fraction, see eq. 4, and the minimum wall thickness, the maximum possible number of fins is 10. For this reason also d_2 is forced to the limit of the constraint.

Table 1. Parametric optimization results.

Parameter	Value
N_{Fin}	10
a	11.464 mm
d_1	0.6050 mm
d_2	0.5000 mm
e_1	0.8576 mm
e_2	2.0105 mm

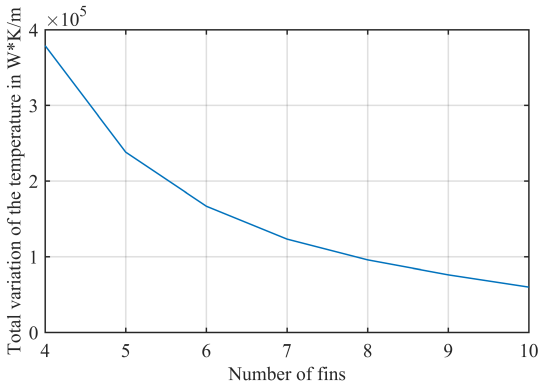

Figure 4. Total variation of the temperature field as a function of the number of fins.

4.2 Topological Model

The results of the topology optimization are shown in Figure 5. Coral-like structures are formed, which become thinner towards the outside. Due to the higher value of the heat source than the heat sink in the simulation, a connection to the outer shell is generated, which is essential for the manufacturability of the component.

The exact position of the surface is determined by a level of ρ_{des}. Figure 5 shows the setting for different levels. Since a defined area fraction γ was specified, the correct choice would be $\rho_{\text{des}} = 0.5$, but it can be observed that this goes along with a discrepancy from the underlying temperature field. A good conformity is achieved at $\rho_{\text{des}} = 0.3$, which is thus used.

As already mentioned, the optimization process will produce some thin, not printable structures, that violate the wall thickness restriction, equation 8. In order to secure an optimal performance of the structure, a procedure to handle these areas needs to be developed, compare with figure 6.

One way (the standard procedure) is to simply not print structures that are smaller than the laser diameter - see Figure 6 dot-dashed line. Since these small structures are located all over the surface,

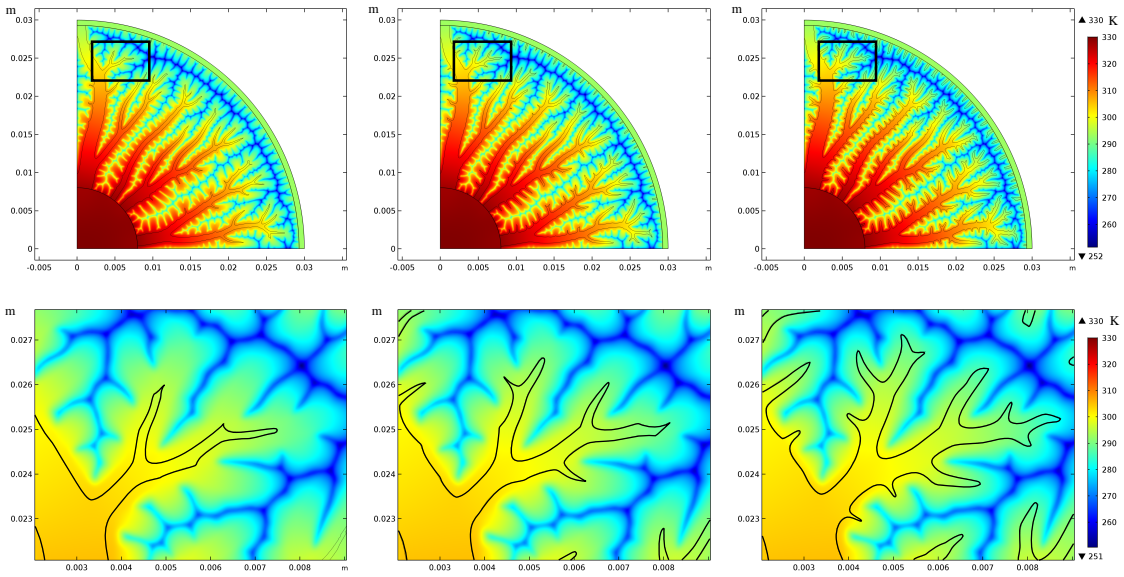

Figure 5. Simulation results with differently chosen surface locations by levels of ρ_{des}, left $\rho_{\text{des}} = 0.5$, middle $\rho_{\text{des}} = 0.4$ and right $\rho_{\text{des}} = 0.3$. The colours represent the temperature field in the domain, the black line shows the location of the surface.

this could reduce the performance of the structure significantly, especially for very small measured devices, since the heat transmission is coupled to the total surface area. On the other hand the weight of the component is further decreased, which can be an important point for lightweight applications.

The other way is to force the laser to expose these thin structures (forced edging - see Figure 6 blue area and dashed line), which results in thickened branches that increase the weight of the structure, while still giving a small loss in performance, compared to the mathematical optimal structure obtained from the optimization.

5. Experiments

In order to validate the numerical results and to compare the optimized designs with each other and conventional designs, as well as the different exposure strategies shown in Figure 6, experiments were carried out.

Three prototypes were manufactured - the parametric optimum, the topological optimum with the normal laser path and the topological optimum with forced edging, compare with Figures 6 and 7. In order to produce structures with high relative densities, a volumetric energy input of around

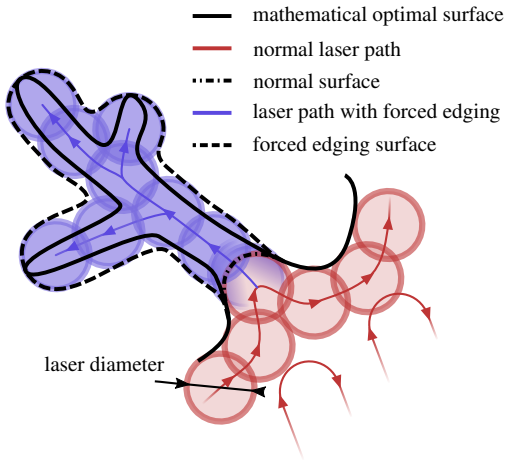

Figure 6. Laserpaths and laser diameter in comparison to the mathematical optimal surface. The red line shows the normal laser path, which will result in neglecting structures smaller than the laser diameter - the resulting structure is represented by the dot-dashed line. The blue line shows the laser path with a forced edging, which results in thickened structures (represented by the dashed line).

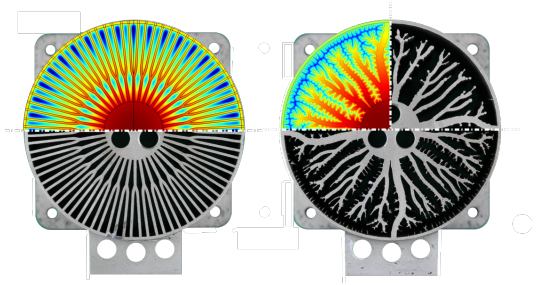

Figure 7. Simulation results and prototypes. Parametric optimum: top - simulation, bottom - printed and post processed part. Topological optimum: upper left - simulation, upper right - printed and post processed part without forced edging. bottom - printed and post processed part with forced edging.

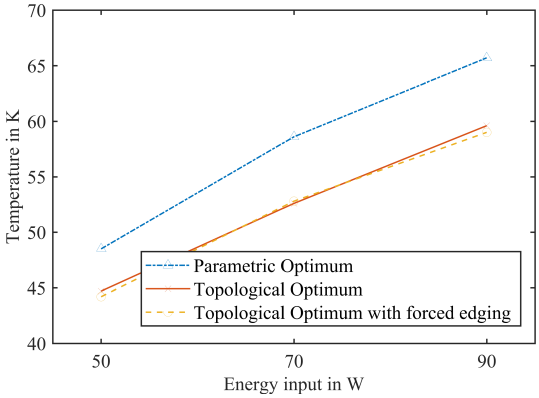

Figure 8. Measured temperature of the prototypes for given wattage (at constant reference temperature).

$340\,\mathrm{J\,m^{-3}}$ was chosen. The parts were produced on an EOS M290 machine with a layer thickness of 60 µm from AlSi10Mg.

Figure 7 shows the simulation results in comparison with the printed and post-processed prototypes.

An experimental setup with a max. 24 V power supply for the heat source and a fan, constantly driven by an additional 12 V power supply, compare with Figure 1, was built up. A thermocouple type K measured the temperature at the heat dissipating component, while a multimeter was used to determine its current draw to calculate the wattage. In order to minimize the influence of measurement errors and hysteresis, multiple measurements were carried out. The results of the measurements are shown in Figure 8. There is a clear performance difference between the parametric and topological models of around 3 to 5 K, gradually increasing with the wattage. A minor difference between the topological prototypes can be observed, with a slightly better performance of the prototype with forced edging.

Table 2. Mass (m), thermal resistance (R_{th}) and weight related thermal resistance (R^*_{th}) of the investigated Prototypes. CON: conventional heat sink, PO: parametric optimum, TO: topological optimum, TOFE: topological optimum with forced edging.

	CON	PO	TO	TOFE
m in kg	0.550	0.170	0.134	0.140
R_{th} in $\mathrm{K\,W^{-1}}$	0.360	0.462	0.376	0.373
R^*_{th} in $\mathrm{K\,kg\,W^{-1}}$	0.198	0.079	0.050	0.053

Table 2 shows the mass and thermal resistance of the investigated prototypes. The conventional heat sink offers the best thermal resistance, which however is accompanied by the greatest weight. The best weight related thermal resistance is achieved by the topological optimum without forced edging, which is around five times better than the conventional component and thus ideally suited for lightweight construction applications. The topological optimum with forced edging has a lower thermal resistance, but since it is a little bit heavier the weighted thermal resistance is higher compared to the topological optimum without forced edging.

6. Conclusions

As expected, the parametric as well as the topological optimization approaches lead to designs with improved performances compared to conventional designs. While the parametric approach has a less costly implementation, the topology approach generates a universal solution, applicable to many familiar problems. Nonetheless the calculation time is much higher due to the need of a finer mesh.

The choice of the exposure strategy (forced edging or not) comes along with slightly different masses and thermal resistances of the optimized

prototypes and should therefore be made in consideration of weight and performance aspects. Because of the easier implementation and shorter calculation times, a parametric optimization is suitable for problems with simple geometries but is accompanied by a loss in performance.

7. References

1. E. M. Dede. Multiphysics topology optimization of heat transfer and fluid flow systems. In *proceedings of the COMSOL Users Conference*, 2009.

2. E. Dede, S. Joshi, and F. Zhou. Topology Optimization, Additive Layer Manufacturing, and Experimental Testing of an Air-Cooled Heat Sink. 137, 07 2015.

3. J. H. K. Haertel, K. Engelbrecht, B. S. Lazarov, and O. Sigmund. Topology optimization of thermal heat sinks. In *Proc. of the 2015 COMSOL Conference, Grenoble*, 2015.

4. J. Alexandersen, O. Sigmund, and N. Aage. Large scale three-dimensional topology optimisation of heat sinks cooled by natural convection. *International Journal of Heat and Mass Transfer*, 100:876 – 891, 2016.

5. M. Zhou, J. Alexandersen, O. Sigmund, and C. B. W. Pedersen. Industrial application of topology optimization for combined conductive and convective heat transfer problems. *Structural and Multidisciplinary Optimization*, 54(4):1045–1060, Oct 2016.

6. M. P. Bendøse and O. Sigmund. Topology Optimization: Theory, Methods and Applications, 2003.

7. C. Emmelmann, P. Sander, J. Kranz, and E. Wycisk. Laser additive manufacturing and bionics: Redefining lightweight design. *Physics Procedia*, 12:364 – 368, 2011. Lasers in Manufacturing 2011 - Proceedings of the Sixth International WLT Conference on Lasers in Manufacturing.

8. R. Neugebauer, B. Müller, M. Gebauer, and T. Töppel. Additive manufacturing boosts efficiency of heat transfer components. *Assembly Automation*, 31(4):344–347, 2011.

9. K. Zander, D. Sokolov, W. Schwarz, and M. Frohnapfel. Scheinwerfer 2025 – bionisch inspiriert und generativ gefertigt. *Lightweight Design*, 9(3):88–93, Jun 2016.

10. J. Kranz, D. Herzog, and C. Emmelmann. Design guidelines for laser additive manufacturing of lightweight structures in TiAl6V4. *Journal of Laser Applications*, 27(S1):S14001, 2015.

11. G. A. O. Adam and D. Zimmer. On design for additive manufacturing: evaluating geometrical limitations. *Rapid Prototyping Journal*, 21(6):662–670, 2015.

12. F. Calignano. Investigation of accuracy and dimensional limits of part produced in aluminum alloy by selective laser melting. *The International Journal of Advanced Manufacturing Technology*, 88(1):451–458, 2017.

13. R. B. Haber, C. S. Jog, and M. P. Bendsøe. A new approach to variable-topology shape design using a constraint on perimeter. *Structural optimization*, 11(1-2):1–12, 1996.

14. E. van de Ven, C. Ayas, M. Langelaar, R. Maas, and F. van Keulen. A PDE-based approach to constrain the minimum overhang angle in topology optimization for additive manufacturing. In *World Congress of Structural and Multidisciplinary Optimisation*, pages 1185–1199. Springer, 2017.

15. L. Shutian, L. Quhao, C. Wenjiong, T. Liyong, and C. Gengdong. An identification method for enclosed voids restriction in manufacturability design for additive manufacturing structures. *Front. Mech. Eng.*, 10(2):126–137, 2015.

16. T. Dbouk. A review about the engineering design of optimal heat transfer systems using topology optimization. *Applied Thermal Engineering*, 112:841–854, 2017.

17. K. Svanberg. The method of moving asymptotes – a new method for structural optimization. *International journal for numerical methods in engineering*, 24(2):359–373, 1987.

18. M. J. D. Powell. The BOBYQA algorithm for bound constrained optimization without derivatives. *Cambridge NA Report NA2009/06, University of Cambridge, Cambridge*, pages 26–46, 2009.

19. S. Cho and J.-Y. Choi. Efficient topology optimization of thermo-elasticity problems using coupled field adjoint sensitivity analysis method. *Finite Elements in Analysis and Design*, 41(15):1481–1495, 2005.